Journal of Geoscience and Environment Protection, 2024, 12, 302-324
https://www.scirp.org/journal/gep
ISSN Online: 2327-4344
ISSN Print: 2327-4336

# Petrology and Petrographic Delineation of Kamlial Formation Sandstone Mong and Thorar Village, Northern Pakistan

**Ehtisham Mehmood[1], Haishen Lv[1*], Pei Gao[1], Soban Qamar[2]**

[1]The National Key Laboratory of Water Disaster Prevention, College of Hydrology and Water Resources, Hohai University, Nanjing, China
[2]College of Mechanical and Petroleum Engineering, University of Engineering and Technology, Taxila, Pakistan
Email: mashuting@hhu.edu.cn, *lvhaishen@hhu.edu.cn, peigao@hhu.edu.cn

**How to cite this paper:** Mehmood, E., Lv, H. S., Gao, P., & Qamar, S. (2024). Petrology and Petrographic Delineation of Kamlial Formation Sandstone Mong and Thorar Village, Northern Pakistan. *Journal of Geoscience and Environment Protection, 12,* 302-324.
https://doi.org/10.4236/gep.2024.125017

**Received:** April 16, 2024
**Accepted:** May 28, 2024
**Published:** May 31, 2024



## Abstract

The origin of sandstone in the Rawalpindi group is disputed because of the lesser Himalayas complicated geological structure and ongoing tectonic activity. The goal of the study is to learn more about the petrographic and geological aspects of the Siwalik molasses deposits, which are formations that belong to the same age group. The Early Miocene Kamlial Formation, the Middle to Late Miocene Chinji Formation, and the Late Miocene Nagri Formation are the stratigraphic units revealed in the project area. The texture of the sandstone found in the Rawalpindi Group and Siwalik is fine to medium-grained. The hue ranges from grey to greenish grey. The sandstone displays thin to medium-bedded layers and exhibits thin lamination throughout. The sandstone of the Kamlial Formation contains load casts, potholes, worm burrows, hematite layers, and filled and unfilled mud cracks in basic structures. Model petrographic research reveals that the Murree Formation primarily consists of light minerals like feldspar, quartzite, and felice, whereas the Kamlial Formation is composed of heavy minerals like garnet and tourmaline. Sandstone from the Rawalpindi group undergoes analysis to ascertain its provenance using the quartz feldspar lithic fragments ternary diagram technique. Each plot in the QFL diagram's recycled orogeny provenance field is plotted.

## Keywords

Hazara Kashmir Syntaxis, Rawalpindi Group, Siwalik Group, Himalayas, Neogene

## 1. Introduction

The project area, nestled in Azad Jammu and Kashmir's District Poonch, between Khirik and Thorar, as delineated by Pakistan's Geological Survey topo-sheet no. 43G/9, boasts coordinates between latitudes 33˚49'30"N and 33˚52'00"N and longitudes 73˚39'00"E and 73˚45'00"E, with an elevation of 1638 meters above sea level (Yasin et al., 2017). Renowned for its breathtaking beauty, Rawalakot, one of Kashmir's most picturesque valleys, lies 80 kilometers equidistant from Rawalpindi and Islamabad, also known as "PEARL VALLEY". The climate in Rawalakot is characterized by four distinct seasons: spring, summer, fall, and winter, with summer temperatures averaging between 25 to 35 degrees Celsius and winter lows dropping to 60 degrees Celsius (Shaheen et al., 2017; Malkani, 2020; Dar & Dubey, 2022).

Geologically, the project region is situated in the Hazara Kashmir Syntaxis (HKS)'s eastern limb, with the Early Miocene Kamlial Formation being a prominent stratigraphic unit in the area (Khan et al., 2024b). The region also features the marine sequence of the Eocene era, housing the Rawalpindi group, a part of the Neogene molasse sequence of the Kohat Plateau. Tectonic forces have led to the tight folding of rocks, resulting in narrow ridges (Hussain et al., 2021). Noteworthy formations in the area include the Chinji, Nagri, Dhok Pathan, and Soan formations of the Siwalik Group, alongside the Murree and Kamlial formations of the Rawalpindi Group, all exposed in the Himalayan foreland Basin (Zaheer et al., 2022).

The Rawalpindi Group, present in the study region, comprises formations like sandstone, siltstone, shales, and conglomerates, indicating less than 18 million years of river deposition, linked to the ancient Indus River (Ali et al., 2019). The Miocene Murree and Kamlial Formations exhibit interbedded shales and sandstones, with distinct color variations and the presence of calcite veins in the sandstone (Javed et al., 2021; Khan et al., 2024a). Petrological studies by (Mughal et al., 2018) have delved into the Murree Formation's petrology, focusing on sandstone and shale characteristics, distinguishing between upper and lower Murree Formations based on grain size.

Previous studies have investigated various sandstone formations in Pakistan, aiming to understand their petrography (Ullah et al., 2006; Abbasi & Yasin, 2017). (Khan et al., 2024c) conducted a detailed petrographic analysis of the Lumshiwal Formation in the Samana Range, Northwestern Pakistan, highlighting provenance, diagenesis, and depositional environments. Similarly, (Abbasi & Yasin, 2017) explored the petrography and diagenetic history of the Nagri Formation sandstone in District Bagh and Muzaffarabad, Pakistan, emphasizing the impact of diagenetic processes on sandstone reservoir quality. Furthermore, (Zaheer et al., 2022) investigated the sandstone petrology and provenance of the Siwalik Group in northwestern Pakistan and western-southeastern Nepal, providing insights into Neogene sedimentary succession and provenance attribution (Khan et al., 2023).

While these studies contribute valuable insights into sandstone petrology and sediment provenance in Pakistan, they primarily focus on mineralogical analysis and

diagenetic processes (Larsen & Chilingarian, 2010; Hashmi et al., 2018; Khan et al., 2024a). In contrast, our research aims to extend this knowledge by conducting a comprehensive petrographic and geochemical analysis of sandstone samples from the Kamlial Formation. By integrating advanced analytical techniques such as scanning electron microscopy (SEM), energy dispersive spectrometry (EDS), and quantitative X-ray diffraction (QXRD), our study offers a detailed characterization of mineralogical composition, diagenetic processes, and sediment provenance in the Kamlial sandstone. This approach enables us to provide a more thorough understanding of the depositional history and hydrocarbon potential of the Kamlial Formation, contributing to the advancement of petroleum geology in Pakistan.

## 2. Stratigraphy of Area

The project area exposes the geological age of molasse deposits. This stratigraphic profile is thoroughly detailed in Table 1 and comprehensively described as follows:

### 2.1. Rawalpindi Group

(Kamran et al., 2010) suggested referring to the rocks containing the Kamlial Formation and Murree Formation in the Kohat-Potwar Province as the Rawalpindi Group, after the Rawalpindi District. The Stratigraphic Committee of Pakistan has confirmed this designation. The group is made up of freshwater-derived shale and sandstone that alternate. While the shale is red and purple, the sandstone is pale to dark red, purple, and grey. The Kamlial Formation's sandstone is distinguished by its abundance of tourmaline and lack of epidote, whereas the Murree Formation's sandstone is distinguished by its excess of epidote. The Rawalpindi Group is widely distributed in Kohat-Potwar Province. According to the Pakistani Stratigraphic Committee (Kamran et al., 2010), the Rawalpindi Group is split into the following two formations:

1) Kamlial Formation

2) Murree Formation (not present in the project area) in the investigation area, Kamlial Formation, is exposed.

### 2.2. Kamlial Formation

Barry et al. (2013) suggested the term "Kamlial Formation", which was subsequently

Table 1. Stratigraphic sequence of the project area.

| | | |
|---|---|---|
| Nagri Formation | Late Miocene | Massive, medium- to coarse-grained sandstone, siltstone, and mudstone with a greenish grey to light-grey color. There are shale and sandstone intermingled. The composition consists of 70% sandstone and 30% shale. |
| Chinji Formation | Middle to Late Miocene | Red to purple, greenish grey shale, purple and reddish-brown mudstone, ash grey sandstone, and siltstone, with 70% clay and 30% sandstone. |
| Kamlial formation | Early to Middle Miocene | Mostly intraformational conglomerates, clays, and sandstone. |

approved by Pakistan's Stratigraphic Committee.

The typical section is a portion in Campbellpur District that is south-west of Kamlial. The medium to coarse-grained, purple-grey, and dark brick-red sandstone that makes up the Kamlial Formation's type section has firm purple shale interbedded with yellow and purple intraformational conglomerate.

## 3. Tectonics of the Project Area

The research area lies in the eastern limb of Hazara-Kashmir Syntaxes (HKS) and represents the northwestern Himalayas as shown in Figure 1. The Himalayas are formed because of collision between Indian and Eurasian plates (Zhang et al., 2012). The HKS is located to the south of Kohistan constitute a great regional bend which has caused inflection of the rocks of the western Himalayas and Hindu Kush (Ali et al., 2016). The HKS is characterized by Panjal Thrust, Main Boundary Thrust, Jhelum fault and Kashmir Boundary Thrust as shown in Figure 1. The tectonic elements of the HKS are described below.

### 3.1. Panjal Thrust

The Panjal Thrust (PT) runs parallel to Main Boundary Thrust (MBT) on the eastern limb of the syntaxis. Left-lateral strike-slip fault truncates the PT and

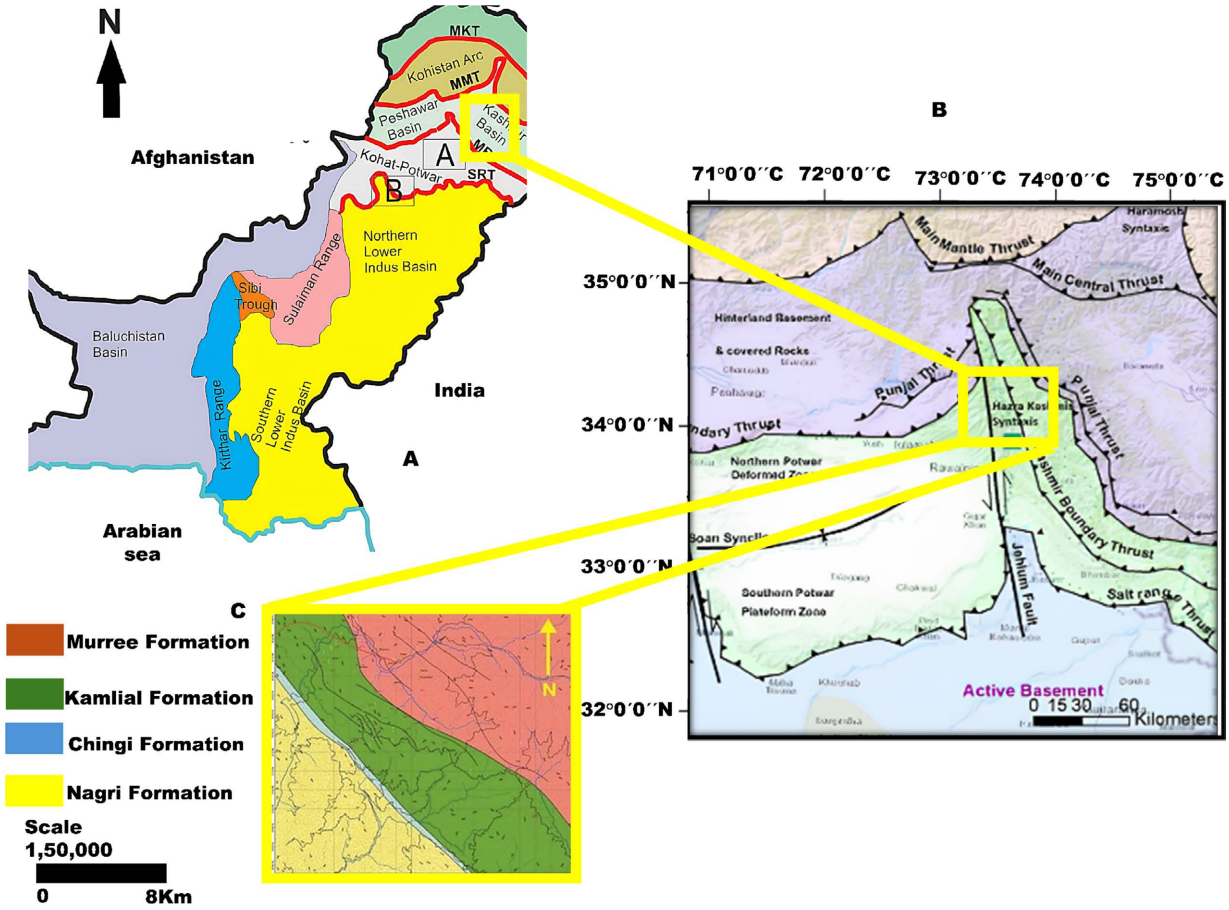


Figure 1. (A) Pakistan's geological map, (B) Northern Pakistan's tectonic map, (C) Scientific map of the research area.

MBT. North of Balakot the PT probably separates from MBT about six kilometers south of Balakot and continues beneath Kunhar valley alluvium up to Gari habib-ullah. The PT and MBT curved around the apex of the HKS. In the eastern limb of HKS, PT runs parallel to the MBT whereas in the western limb MBT follows an oblique course.

### 3.2. Main Boundary Thrust (MBT)

The Main Boundary Thrust (MBT) separates the lesser Himalayan pre-collision in the eastern limb of HKS from west to east Murree Thrust, Koral Thrust, Kathmandu Thrust and Gondwana Thrust are generally considered as the continuation of MBT. In this area MBT is less deform as compared to the western limb where a series of southeast verging parallel thrust faults (NE-SW to E-W) off shoot from the northwest trending strike-slip JF along the river Jhelum (Singh & Patel, 2022). Literature survey suggested the name of Murree Thrust on both the limbs of HKS as the MBT (Ali et al., 2015).

### 3.3. Kashmir Boundary Thrust

The Kashmir Boundary Thrust (KBT) is now also known as Balakot Bagh Fault (Shah, 2015). The rupture zone passes through Balakot, Muzaffarabad, Kardalla, Bandi Karim Haidershah, Sarain, Chikar and Sudhangali. Medium to long range earthquakes is expected in the study area. This fault is between Abbottabad Formation (Cambrian) and Murree Formation (Miocene) (Dar & Dubey, 2022).

## 4. Methodology

### 4.1. Materials and Methods

#### 4.1.1. Description of the Kamlial Formation

The Kamlial Formation, predominant in the project area (as shown in **Figure 2**), comprises secondary clays, siltstone, and sandstone. Notably, the sandstone exhibits a greyish coloration with a medium-grained, compact, and firm texture, often occurring in massive and laminated layers within the formation.

#### 4.1.2. Geological Fieldwork

Two weeks of intensive geological fieldwork were conducted to gather primary data. This involved the use of Global Positioning System (GPS) and Brunton Compass for accurate spatial data collection (as shown in **Figure 3**).

#### 4.1.3. Geological Mapping

Comprehensive geological maps of the study area were prepared based on field observations and data collected during the fieldwork. These maps, depicted in **Figure 2** and **Figure 3**, serve as foundational resources for the study.

#### 4.1.4. Sample Collection and Preparation

Sixteen representative rock samples of sandstone were meticulously collected across the study area. Sample locations were chosen based on a thorough analysis of rock characteristics, including color, texture, structure, joints, and thickness.

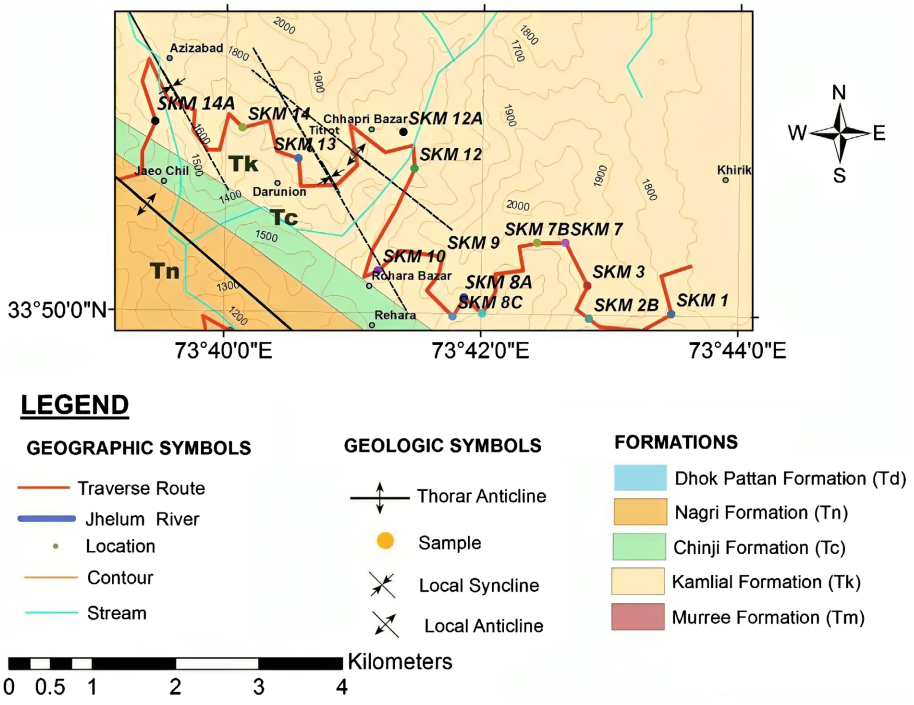


Figure 2. Sample location map of Khirik to Thorar area.

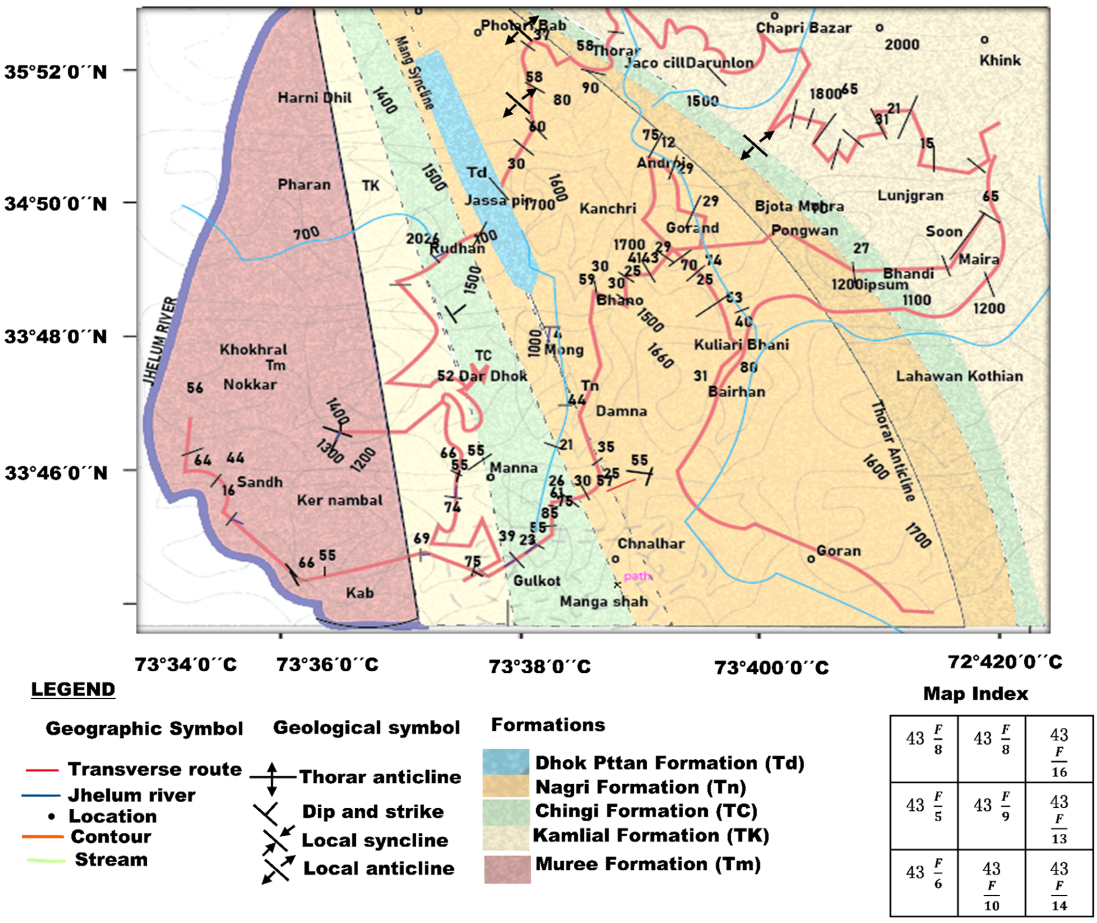


Figure 3. Geological field samples map of Khrick and Mong area.

Samples were named according to a standardized convention (e.g., SKM), denoting the type of rock and its location.

#### 4.1.5. Laboratory Analysis

Thin sections of the collected sandstone samples were prepared at the Geoscience Laboratory in Islamabad. These thin sections were examined under a petrographic microscope, specifically a Leica DM750P, equipped with a 4× to 40× magnification capability and an attached Leica EC3 camera linked to a computer for detailed analysis.

#### 4.1.6. Objective of Petrography

The primary objective of the study is to conduct petrographic analysis of the sandstone within the Kamlial Formation. This analysis aims to determine the provenance of the sandstone and unravel its depositional history.

#### 4.1.7. Base Map Creation

A base map at a scale of 1:50,000 was meticulously crafted by enlarging the relevant portions of Survey of Pakistan toposheets 43G/9 and 43G/13 four times. This base map serves as a crucial reference for recording field observations and sampling locations.

#### 4.1.8. Field Observations and Mapping

Traverses across the strike were systematically conducted during fieldwork to capture variations in sedimentary facies. Field observations, including dips, strikes, joints, and fissures, were meticulously recorded on the base map to facilitate the creation of a detailed geological map.

#### 4.1.9. Sampling Strategy and Bias Mitigation

Samples were selectively taken from newly formed outcrops, avoiding mechanically or chemically worn locations to mitigate potential sampling biases. This approach ensures the collection of fresh, representative samples for accurate analysis.

#### 4.1.10. Data Integration and Quality Control

Field data collected during geological mapping were integrated with base maps to enhance accuracy and detail. Quality control measures were implemented during mapping to minimize errors and ensure the reliability of data.

## 5. Petrology

Only sedimentary rocks were included in the petrographic analysis. Sandstone samples, both new and representative, were collected from well-exposed rock units within the study area. In the lab, the thin sections were produced and examined under a microscope. Tables 2-4 give the modal mineralogical data of rocks. The texture of the sandstone in the Rawalpindi Group and Siwalik is fine to medium-grained. The color varies from greenish grey to grey. The sandstone is thinly laminated, thin to medium bedded. In primary structures, load casts,

**Table 2.** Modal mineralogy of lithic arenites.

| Modal Mineralogical composition | | | Sample slide Numbers | | | | |
|---|---|---|---|---|---|---|---|
| | | | SKM 7 | SKM 10 | SKM 12 | SKM 12-A | SKM 14 |
| Quartz | Monocrystalline Quartz | | 30 | 26 | 28 | 21 | 25 |
| | Polycrystalline Quartz | | 3 | 5 | 2 | 6 | 2 |
| Feldspar | Perthite | | -- | -- | 1 | -- | -- |
| | Microcline | | -- | 1 | -- | 2 | 3 |
| | Microcline-perthite | | -- | -- | 1 | -- | -- |
| | Plagioclase | | 2 | 2 | 0.5 | 1 | 1 |
| Rock Fragments | Sandstone | | 3.5 | 5 | 2 | 5 | 5 |
| | Sedimentary | Siltstone | 3 | 4 | 3 | 5 | 6 |
| | | Limestone | 3 | 4 | 3 | 4 | 4 |
| | Metamorphic | Quartzite | 2 | 4 | 3 | 3 | 4 |
| | | Slate | 2 | 4 | 5 | -- | 2 |
| | | Schist | 5 | 4 | 3 | 4 | 3 |
| | Igneous | Volcanic | -- | 7 | -- | 5 | -- |
| | Muscovite | | 4 | 3 | 5 | 2 | 6 |
| | Biotite | | 5 | 1 | 3 | 3 | 3 |
| Accessory minerals | Tourmaline | | 1 | -- | 1 | 1 | 1 |
| | Hornblende | | -- | -- | -- | 1 | -- |
| | Epidote | | -- | -- | 0.4 | 1 | -- |
| | Chlorite | | 2 | 1 | 2 | 1 | 2.6 |
| | Hematite | | 2.5 | -- | 1 | -- | 1 |
| | Sericite | | -- | -- | 0.1 | -- | 0.4 |
| | Opaque | | 3 | 3 | 4 | 2 | 2 |
| Cementing material Matric | Calcite | | 24 | 22 | 27 | 27 | 25 |
| | Hematite | | 1 | -- | 1 | 2 | 1 |
| | Arenite | | 4 | 4 | 4 | 4 | 3 |

**Table 3.** Modal mineralogy of lithic wacke.

| Modal Mineralogical composition | | Sample Slide Numbers | | | | | |
|---|---|---|---|---|---|---|---|
| | | SKM 1 | SKM 2-B | SKM 3 | SKM 7-B | SKM 8-A | SKM 8-B |
| Quartz | Monocrystalline Quartz | 22 | 25 | 25 | 27 | 25 | 26 |
| | Polycrystalline Quartz | 8 | 5 | 2 | 7 | 5 | 5 |
| Feldspar | Perthite | -- | -- | 1 | 1 | -- | -- |
| | Microcline | 1.5 | -- | 1 | -- | 1 | 2 |

**Continued**

| | | | | | | | | |
|---|---|---|---|---|---|---|---|---|
| | Microcline-perthite | | -- | -- | 1 | -- | 1 | -- |
| | Plagioclase | | 1.5 | 4 | 2 | 2.5 | 3 | 1 |
| Rock Fragments | Sedimentary | Sandstone | 7 | 2 | 4 | 2 | 6 | 4 |
| | | Siltstone | 6 | 3 | 3 | 5 | 7 | 6 |
| | | Limestone | 2 | 4 | 2 | | 2 | 3 |
| | Metamorphic | Quartzite | 2 | 3 | 3 | 3 | 3 | 3 |
| | | Slate | 5 | 2 | 4 | 4 | 6 | 3 |
| | | Schist | 4 | 6 | 3 | 3 | 4 | 4 |
| | Igneous | Volcanic | 4 | 2 | -- | 6 | -- | 6 |
| | Muscovite | | 4 | 3 | 3 | 4 | 3 | 3 |
| | Biotite | | 3 | 3 | 4 | 5 | 4 | 1 |
| Accessory minerals | Tourmaline | | 1 | 1 | -- | 1 | -- | -- |
| | Chlorite | | 2 | 1 | -- | -- | 2 | -- |
| | Hematite | | 2 | 4 | -- | 2 | -- | 1 |
| | Sericite | | -- | -- | -- | 0.5 | -- | -- |
| | Opaque | | 16 | 20 | 28 | 15 | 19 | 21 |
| Cementing material | Calcite | | -- | 2 | 3 | -- | 1 | 1 |
| | Hematite | | -- | 2 | 3 | -- | 1 | 1 |
| | Wacke | | 7 | 7 | 7 | 8 | 6 | 7 |

**Table 4.** Modal mineralogy of lithic wacke.

| Modal Mineralogical composition | | | Sample slide Numbers | | | | |
|---|---|---|---|---|---|---|---|
| | | | SKM 8-C | SKM 9 | SKM 12-B | SKM 13 | SKM 14-A |
| Quartz | Monocrystalline Quartz | | 26 | 25 | 28 | 22 | 26 |
| | Polycrystalline Quartz | | 2 | 6 | 4 | 5 | 4 |
| Feldspar | Perthite | | 1 | -- | 1 | 1 | -- |
| | Microcline | | -- | 2 | -- | -- | |
| | Plagioclase | | 3 | 2 | -- | 2 | 3 |
| Rock Fragments | Sedimentary | Sandstone | 3 | 6 | 3 | 4 | 3 |
| | | Siltstone | 4 | 3 | 3 | 6 | 2 |
| | | Limestone | -- | -- | 2 | -- | 3 |
| | Metamorphic | Quartzite | 4 | 1 | 2 | -- | 2 |
| | | Slate | 6 | 2 | 3 | 8 | 2 |
| | | Schist | 6 | 2 | 4 | 2 | 7 |
| | Igneous | Volcanic | 6 | -- | 2 | 5 | 2 |

**Continued**

| | | | | | | |
|---|---|---|---|---|---|---|
| | Muscovite | 3 | 4 | 3 | 3 | 2 |
| | Biotite | 2 | 3 | 6 | 3 | 2 |
| Accessory minerals | Tourmaline | -- | 1 | -- | | 0.5 |
| | Epidote | -- | -- | 1 | -- | 0.5 |
| | Garnet | -- | -- | -- | -- | -- |
| | Chlorite | 2 | -- | -- | 2 | 1 |
| | Hematite | 2 | 3 | 3 | -- | -- |
| | Opaque | | 7 | 3 | 4 | 5 |
| Cementing material | Calcite | 18 | 27 | 22 | 25 | 26 |
| | Hematite | 3 | -- | 2 | 1 | 2 |
| | Wacke | 9 | 6 | 8 | 7 | 7 |


**Figure 4.** Slump folding in sandstone.


**Figure 5.** Photograph shows laminated Kamlial.

potholes, hematite layers and worm burrows (as shown in **Figure 8**) are found in Kamlial Formation. Calcite concretion (as shown in **Figure 9**), hematite concretion (as shown in **Figure 6**), and filled and unfilled mud cracks are also found in the sandstone of the Kamlial Formation. Massive sandstone and shale

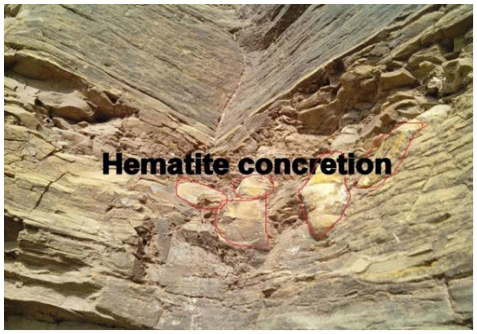


Figure 6. Hematite concentration in Kamlial formation.

Figure 7. Photograph shows clasts of quartzite.

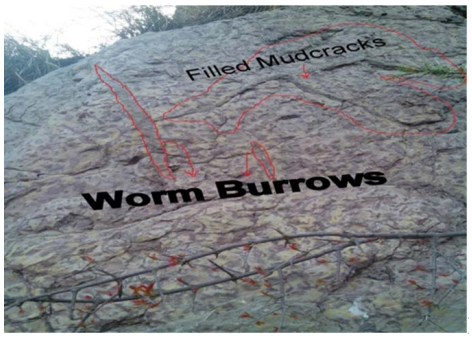


Figure 8. Photograph shows laminated worm burrows.


Figure 9. Photograph shows calcite concretion.

beds and conglomerates, micro conglomerates between sandstone beds, and laminated sandstone (as shown in Figure 5) and slump folding in sandstones (as shown in Figure 4). Local anticlines near Chappri Bazar are found in the Kamli-

al Formation. Intraformational clasts such as quartzite clast (as shown in Figure 7) are also found in the Kamlial Formation.

### 5.1. Microscopic Features of SKM 7 (Lithic Arenite)

In SKM 7, the quartz grains exhibit a predominantly sub-angular to sub-round shape, with a minority displaying angular and stretched characteristics. Notably, unstrained quartz predominates over strained metamorphic quartz. Some quartz grains display fractures, while the contact between quartz grains is primarily planar. Monocrystalline quartz prevails over polycrystalline quartz, comprising 30% and 3% of the sample, respectively. Additionally, feldspar grains, including plagioclase, constitute 2% of the rock sample, with plagioclases appearing sub-angular in shape. Sedimentary rock fragments, including siltstone (3%), sandstone (3.5%), and limestone (3%), are present. Metamorphic rock fragments include quartzite (2%), slate (2%), and schist (5%). Accessory minerals encompass muscovite (4%), biotite (5%), tourmaline (1%), opaque minerals (3%), chlorite (2%), and hematite (2.5%). Cementing materials include calcite (24%) and hematite (1%). The matrix content is 4%, classifying the sample as arenite as shown in Table 2.

### 5.2. Microscopic Features of SKM 12 (Lithic Arenite)

Similarly, in SKM 12, quartz grains display a sub-angular to sub-round shape, with some exhibiting angular and stretched characteristics. Unstrained quartz predominates over strained metamorphic quartz, with a few fractured grains. The contact between quartz grains is primarily planar. Monocrystalline quartz prevails over polycrystalline quartz, comprising 28% and 2% of the sample, respectively. Feldspar grains include plagioclase (0.5%), perthite, and microcline-perthite (1%), with plagioclases appearing sub-rounded in shape, perthite angular, and microcline sub-angular to sub-round. Sedimentary rock fragments consist of siltstone (3%), sandstone (2%), and limestone (3%). Metamorphic rock fragments include quartzite (3%), slate (5%), and schist (3%). Accessory minerals encompass muscovite (4%), biotite (5%), tourmaline (1%), opaque minerals (3%), chlorite (2%), and hematite (2.5%). Cementing materials include calcite (24%) and hematite (1%) as shown in Table 2.

### 5.3. Microscopic Features of SKM 12A (Lithic Arenite)

In SKM 12A, quartz grains exhibit a sub-angular to sub-round shape, with some displaying angular and stretched characteristics. Unstrained quartz prevails over strained metamorphic quartz, with a few fractured grains. The contact between quartz grains includes planar and point contacts (as shown in Figures 10-17). Monocrystalline quartz is more abundant than polycrystalline quartz, comprising 21% and 6% of the sample, respectively. Feldspar grains, including plagioclase (1%) and microcline (2%), exhibit shapes ranging from sub-angular to sub-round. Sedimentary rock fragments include limestone (4%), sandstone (5%), and siltstone (5%) (as shown in Figure 16). Accessory minerals encompass muscovite

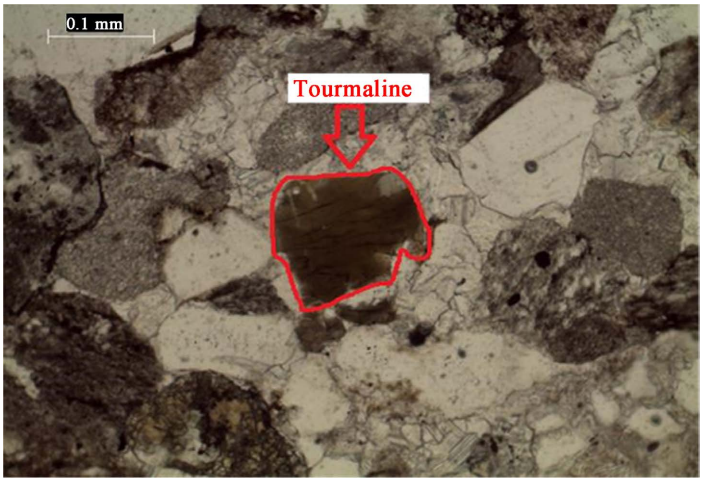


**Figure 10.** Photomicrograph shows tourmaline in lithic arenite of Kamlial Formation (SKM 12A, (Cross Nicol: 10×).

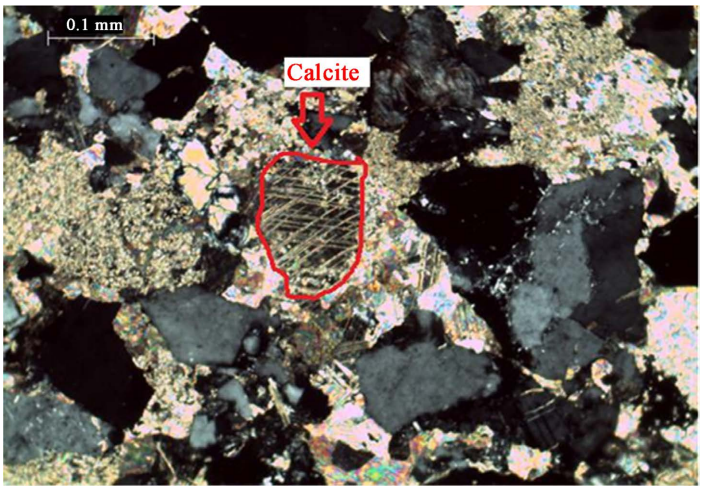


**Figure 11.** Photomicrograph shows calcite cement in crystal in lithic arenite of Kamlial Formation (SKM 12A), (PPL: 10×).

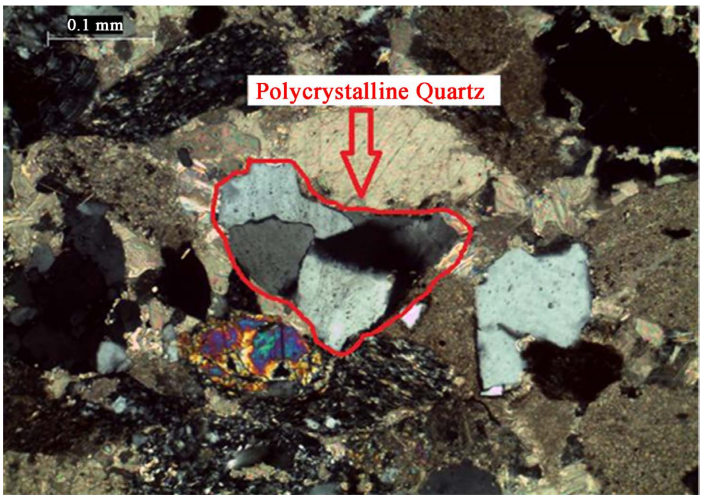


**Figure 12.** Photomicrograph shows polycrystalline quartz in lithic arenite of Kamlial Formation (SKM 12A), (Cross Nicol: 10×).

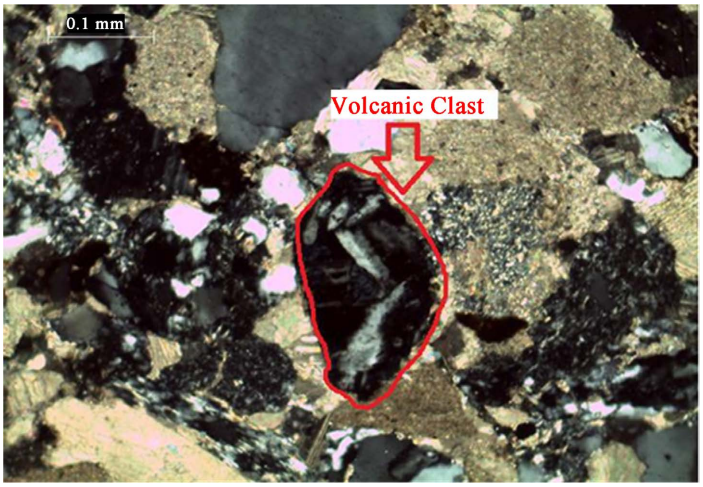


Figure 13. Photomicrograph shows calcite cement in crystal in lithic arenite of Kamlial Formation (SKM 12A), (PPL: 10×).

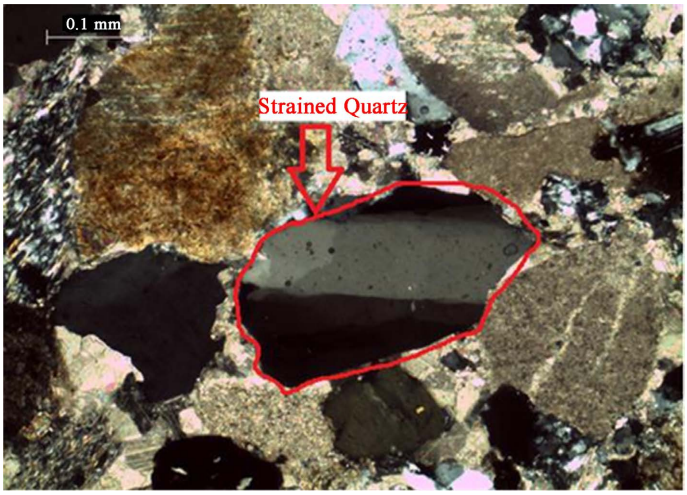


Figure 14. Photomicrograph shows strained quartz in lithic arenite of Kamlial Formation (SKM 12A), (Cross N), (l: 10×).


Figure 15. Photomicrograph shows muscovite in in crystal in lithic arenite of Kamlial Formation (SKM 12A), (PPL: 10×).

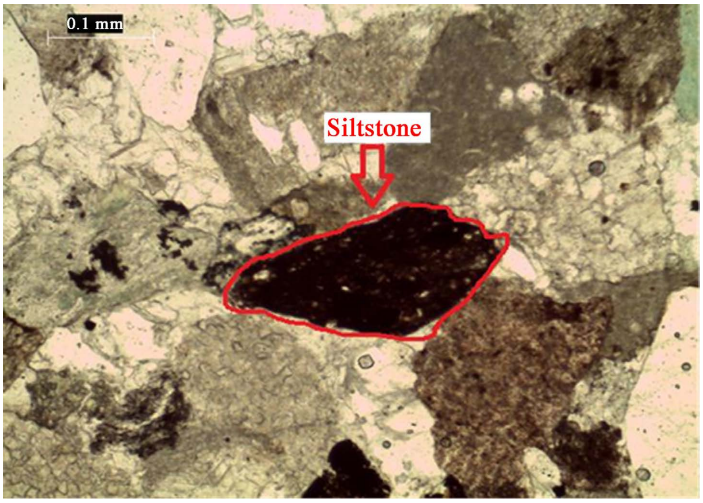


Figure 16. Photomicrograph shows siltstone in lithic arenite of Kamlial Formation (SKM 12A), (Cross Nicol: 10×).

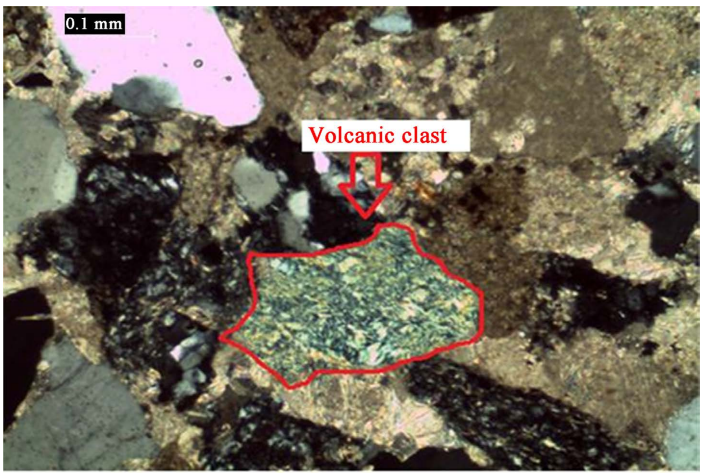


Figure 17. Photomicrograph shows volcanic clast in crystal in lithic arenite of Kamlial Formation (SKM 12A), (PPL: 10×).

(4%), biotite (5%), tourmaline (1%), opaque minerals (3%), chlorite (2%), and hematite (2.5%) as shown in Table 2.

The classification of samples extracted from the Kamlial Formation (Legend Arenites) as shown in Figure 18, spanning from Khirik to Thorar within the project area. Utilizing the classification scheme proposed by Yasin et al. 2017, the samples are categorized into three distinct types: quartz wacke (labeled a), feldspathic wacke (b), and lithic wacke (c). Given that the Kamlial Formation predominantly consists of quartz and lithic components, it is notable that a significant portion of the samples falls within the quartz and lithic regions of the diagram.

### 5.4. Microscopic Features of SKM 1 (Lithic Wacke)

Quartz is sub-angular to sub-round in shape and few grains are angular. Unstrained igneous is more than strained metamorphic quartz. Few quartz grains

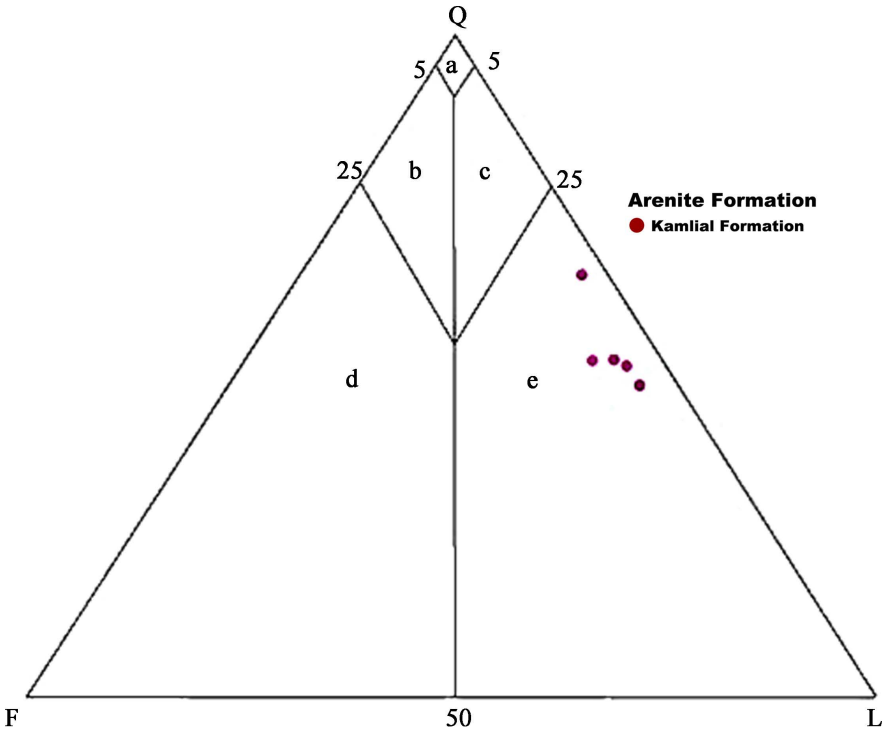


Figure 18. Classification of samples from the Kamlial Formation in the project area from Khirik to Thorar. Field boundaries are after Yasin et al., 2017, where a = quartz wacke, b = feldspathic wacke, and c = lithic wacke.

are starched. The contact between quartz is planer and point contact. Monocrystalline quartz is more than polycrystalline quartz. Monocrystalline quartz is 22% while polycrystalline is 8% in this sample as shown in Table 3 & Table 4. Feldspar grains include plagioclase constitute 1.5% and microcline 1.5% in the rock sample. Plagioclases are sub-angular while microcline is sub-rounded in shape.

### 5.5. Microscopic Features of SKM 2B (Lithic Wacke)

Quartz is sub-angular to sub-round in shape and a few grains are angular and stretched. Unstrained quartz is more than strained metamorphic quartz. Few quartz grains are fractured. The contact between quartz is planer contact. Monocrystalline quartz is more than polycrystalline quartz. Monocrystalline quartz are 25% while polycrystalline is 5% in sample SKM 2B as shown in Table 3 & Table 4. Feldspar grains include plagioclase constitute 4% in the rock sample. Plagioclases are sub-angular in shape.

### 5.6. Microscopic Features of SKM 7-B (Lithic Wacke)

Quartz is sub-angular to sub-round in shape and few grains are angular and stretched. Unstrained quartz is more than strained metamorphic quartz. Few quartz grains are fractured. The contact between quartz is planer contact and point contact. Monocrystalline quartz is more than polycrystalline quartz. Mo-

nocrystalline quartz is 27% while polycrystalline is 7% in this sample as shown in Table 3 & Table 4. Feldspar grains include plagioclase constitute 2.5% and perthite 1% in the rock sample. Plagioclase and perthite are sub-angular to sub-rounded in shape.

The detailed examination of these photomicrographs (as shown in Figures 19-22) reveals crucial information about the mineral composition and texture of the rock samples. The presence of green biotite, as evidenced in the first and second images, indicates the occurrence of mafic minerals within the studied specimens. Meanwhile, the identification of muscovite in the fourth image suggests the presence of phyllosilicates, offering insights into the rock's geological history. Additionally, the observation of siltstone in the third image signifies the sedimentary nature of the rock, providing valuable clues about its depositional

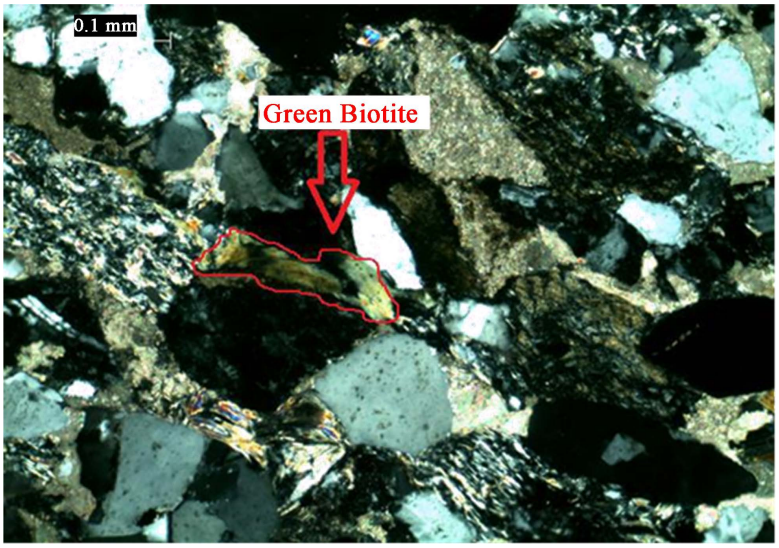


Figure 19. Photomicrograp shows green biotite.

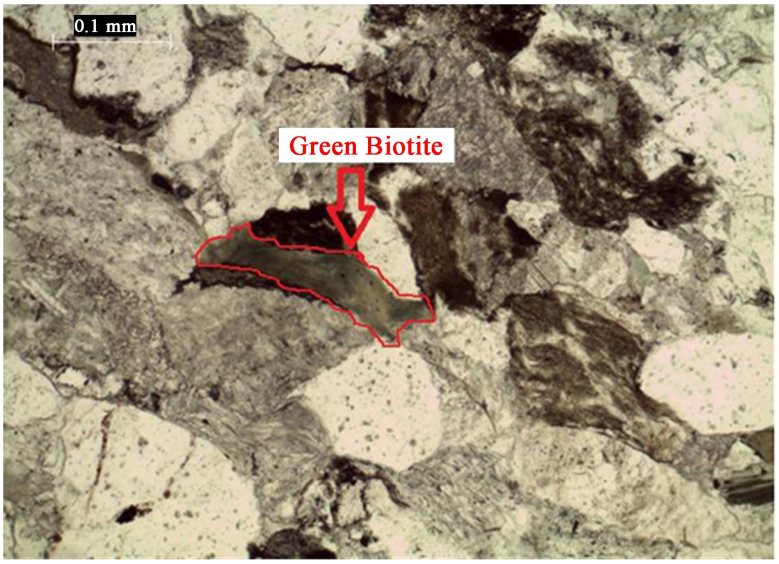


Figure 20. Photomicrograph shows green biotite.


Figure 21. Photomicrograph shows siltstone clast.

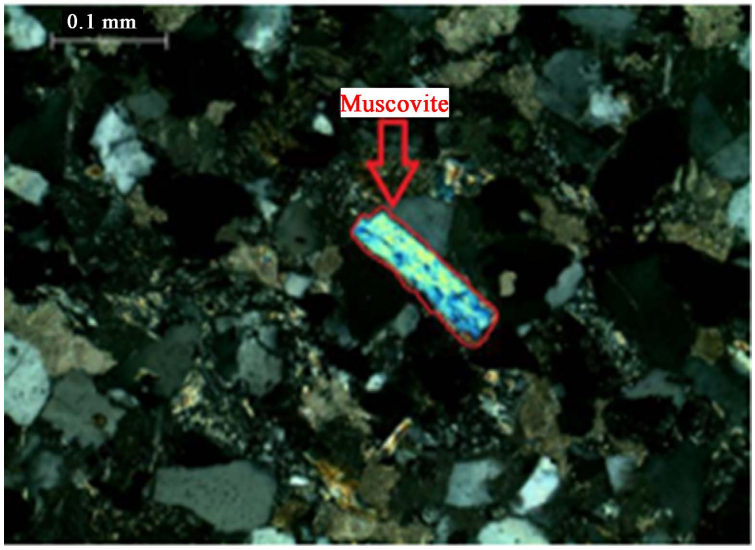


Figure 22. Photomicrograph shows muscovite flake.

environment. These findings contribute significantly to our understanding of the geological formations under investigation and their broader geological implications.

Figure 23 illustrates a hypothetical model showcasing the collision between the Indian and Eurasian plates, which led to the formation of the foreland basin. This visual representation effectively portrays the complex tectonic processes involved in plate convergence and basin development, providing valuable insights into the geological evolution of the region. Furthermore, In Figure 24, we observe a hypothetical scenario depicting the collision between the Indian and Eurasian plates. This collision is pivotal in generating the foreland basin, as showcased in the diagram. By illustrating this geological process, the figure offers valuable insights into the dynamics of plate tectonics and basin formation.

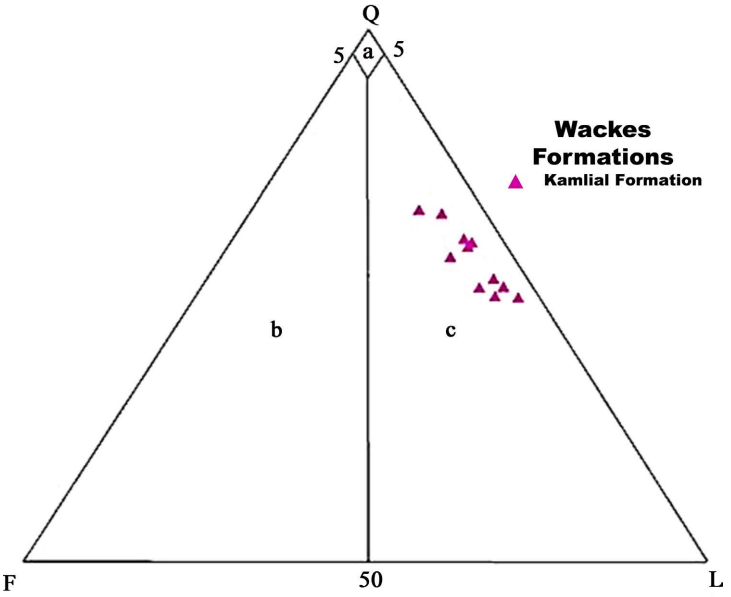


Figure 23. Classification of sandstone samples of Kamlial Formation in the project area from Khirik to Thorar. Field boundaries are after Yasin et al., 2017, where a = Quartz wacke, b = Feldspathic wacke, c = Lithic wacke.

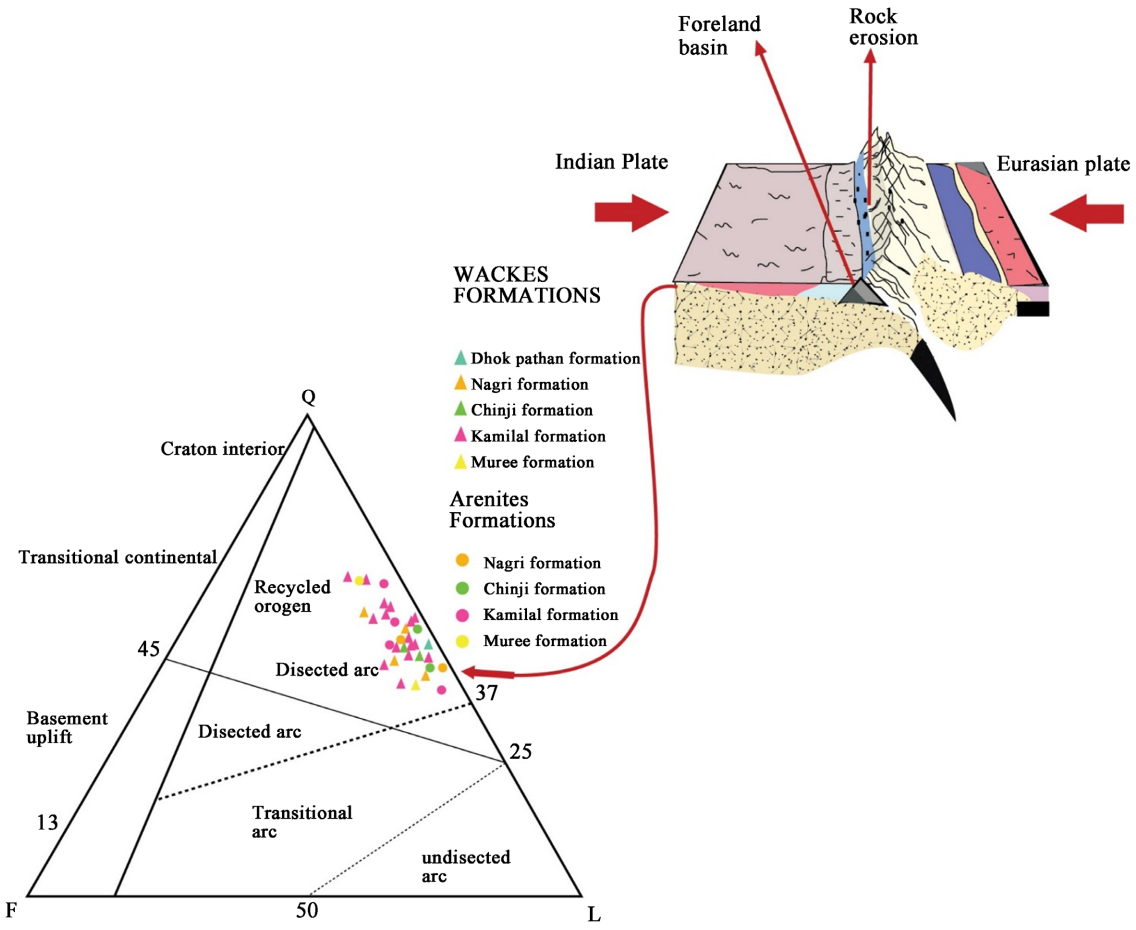


Figure 24. Hypothetical Modal demonstrates how the Indian and Eurasian plates collided with one another to generate the foreland basin.

## 6. Provenance Analysis

In the detailed analysis conducted on the sandstone sourced from the Kamlial Formation, an exhaustive investigation into its provenance has been precisely carried out, revealing invaluable insights into its geological origins. The diverse range of quartz grains, showcasing a spectrum of morphologies from sub-angular to sub-round, interspersed with occasional angular and stretched features, serves as pivotal evidence shedding light on the sedimentary processes that have shaped the sandstone over time. Notably, the observations of both strained and unstrained grains further deepen our understanding of the dynamic depositional environment that influenced the sandstone's formation. Furthermore, the identification and characterization of feldspar minerals within the sandstone, including the discernment of plagioclase, perthite, and microcline, offer significant indications of the diverse array of source rock compositions contributing to the sandstone's genesis. Through this comprehensive mineralogical analysis, we gain valuable insights into the complex interplay of geological factors that have culminated in the formation of sandstone.

Moreover, the recognition of various rock fragment types, spanning a wide spectrum of sedimentary, metamorphic, and igneous origins, is paramount for unraveling the intricate depositional history of the sandstone and elucidating its provenance. The presence of accessory minerals such as tourmaline, hornblende, epidote, chlorite, hematite, sericite, and opaque minerals further enriches the analysis, serving as critical indicators of the geological processes and source materials involved in the sandstone's formation (Khan et al., 2024c). Additionally, the identification of calcite and hematite as primary cementing materials provides illuminating insights into the diagenetic processes responsible for the consolidation of the sandstone, thereby augmenting our comprehension of its post-depositional alterations.

### Comparison between Provenance and QFL Analysis

Comparing provenance analysis with QFL analysis reveals distinct approaches and perspectives in understanding sedimentary rocks' origins. Provenance analysis focuses on deciphering the source regions of sedimentary deposits by examining mineralogical composition, rock fragment types, and accessory minerals (Cheng et al., 2019; Khan et al., 2024c). This method provides detailed insights into the geological processes and environments responsible for sediment formation. In contrast, QFL analysis primarily quantifies the relative abundance of quartz, feldspar, and lithic fragments in sedimentary rocks, offering a simplified yet quantitative assessment of sediment composition (Huber & Bahlburg, 2021). While provenance analysis offers a more comprehensive understanding of depositional history and source materials, QFL analysis provides a quick and standardized method for characterizing sedimentary rocks, particularly in large-scale studies or when detailed mineralogical data is not required (Hussain et al., 2021). Each approach has its advantages and limitations, making them complementary

tools in sedimentary geology research.

## 7. Conclusion

In conclusion, our study of the Kamlial Formation's sandstone has yielded several significant insights into the geological dynamics of the Sub-Himalayan Hazara Kashmir Syntaxis. We have identified a gradual transition between Siwalik and Rawalpindi group formations in the Khirik and Thorar districts of Poonch, along with the absence of key formations in the project region. The presence of intraformational microconglomerates and hematite concretions suggests a shift towards arid and semiarid environmental conditions in the Himalayan foreland basin. Tectonic forces have played a crucial role, formed a thorium anticline and influencing regional geological structures. Our detailed petrological analysis has delineated distinct lithic wacke and lithic arenite facies, providing valuable insights into their composition and origin. Additionally, the diversity in quartz grain shapes indicates a complex sedimentary history, with contributions from both proximal and distal sources. The presence of interformational and intraformational clasts further emphasizes the composite nature of sedimentary deposition in the region. Moving forward, our findings have implications for broader geological and environmental studies in the Himalayan foreland basin. Future research efforts could focus on refining provenance analysis techniques and exploring the wider implications of these discoveries for understanding the dynamic geological processes shaping the region.

## Funding

This work was supported by the National Natural Science Foundation of China (41830752, 42071033).

## Conflicts of Interest

The authors declare no conflicts of interest regarding the publication of this paper.

## References

Abbasi, N., & Yasin, M. (2017). Petrography and Diagenetic History of Nagri Formation Sandstone in District Bagh and Muzaffarabad, Pakistan. *Pakistan Journal of Geology, 1,* 21-23. https://doi.org/10.26480/pjg.02.2017.21.23

Ali, A., Faisal, S., Rehman, K. et al. (2015). Tectonic Imprints of the Hazara Kashmir Syntaxis on the Northwest Himalayan Fold and Thrust Belt, North Pakistan. *Arabian Journal of Geosciences, 8,* 9857-9876. https://doi.org/10.1007/s12517-015-1874-8

Ali, A., Pan, J., Yan, J., & Nabi, A. (2019). Lithofacies Analysis and Economic Mineral Potential of a Braided Fluvial Succession of NW Himalayan Foreland Basin Pakistan. *Arabian Journal of Geosciences, 12,* Article No. 222. https://doi.org/10.1007/s12517-019-4295-2

Ali, A., Yar, M., Khan, M. A., & Faisal, S. (2016). Interrelationships between Deformation and Metamorphic Events across the Western Hinterland Zone, NW Pakistan. *Journal*

*of Earth Science, 27,* 584-598. https://doi.org/10.1007/s12583-016-0717-1

Barry, J. C., Behrensmeyer, A. K., Badgley, C. E. et al. (2013). Chapter 15. The Neogene Siwaliks of the Potwar Plateau, Pakistan. In X. Wang, L. J. Flynn, & M. Fortelius (Eds.), *Fossil Mammals of Asia* (pp. 373-399). Columbia University Press. https://doi.org/10.7312/wang15012-015

Cheng, F., Garzione, C., Jolivet, M. et al. (2019). Provenance Analysis of the Yumen Basin and Northern Qilian Shan: Implications for the Pre-Collisional Paleogeography in the NE Tibetan Plateau and Eastern Termination of Altyn Tagh Fault. *Gondwana Research, 65,* 156-171. https://doi.org/10.1016/j.gr.2018.08.009

Dar, J. A., & Dubey, R. K. (2022). Sediment Deformational Structures in Quaternary Sediment Sequences of Kashmir Basin India, with Special Reference to Microstructures. *Quaternary Science Advances, 5,* Article ID: 100040. https://doi.org/10.1016/j.qsa.2021.100040

Hashmi, S. I., Jan, I. U., Khan, S., & Ali, N. (2018). Depositional, Diagenetic and Sequence Stratigraphic Controls on the Reservoir Potential of the Cretaceous Chichali and Lumshiwal Formations, Nizampur Basin, Pakistan. *Journal of Himalayan Earth Sciences, 51,* 44-65.

Huber, B., & Bahlburg, H. (2021). The Provenance Signal of Climate-Tectonic Interactions in the Evolving St. Elias Orogen: Framework Component Analysis and Pyroxene and Epidote Single Grain Geochemistry of Sediments from IODP 341 Sites U1417 and U1418. *International Journal of Earth Sciences (Geologische Rundschau), 110,* 1477-1499. https://doi.org/10.1007/s00531-021-02025-9

Hussain, S. M., Hussain, S. K., & Meybodi, E. E. (2021). Petrographic and Provenance of the Sandstone of Rawalpindi Group in Lesser Himalayas. *Earth Sciences Malaysia (ESMY), 5,* 93-103. https://doi.org/10.26480/esmy.02.2021.93.103

Javed, A., Wahid, A., Mughal, M. S. et al. (2021). Geological and Petrographic Investigations of the Miocene Molasse Deposits in Sub-Himalayas, District Sudhnati, Pakistan. *Arabian Journal of Geosciences, 14,* 1-24.

Kamran, S. M., Khan, M. S., & Siddiqi, M. I. (2010). Petrography of Sandstone of Molasse Deposits (Rawalpindi Group) and Their Tectonic Setting from Khairi-Murat Area, Potwar Sub-Basin, Pakistan. *Pakistan Journal of Hydrocarbon Research, 20,* 15-25.

Khan, M. A., Mahato, S., Spicer, R. A. et al. (2023). Siwalik Plant Megafossil Diversity in the Eastern Himalayas: A Review. *Plant Diversity, 45,* 243-264. https://doi.org/10.1016/j.pld.2022.12.003

Khan, M. W., Rehman, S. U., Ahmed, S., & Sameeni, S. J. (2024c). Provenance of the Lower Cretaceous Lumshiwal Formation, Surghar Range, Northwestern Indian Plate, Pakistan: Insights from New Petrographical and Geochemical Analysis. *Journal of Asian Earth Sciences: X, 11,* Article ID: 100172. https://doi.org/10.1016/j.jaesx.2023.100172

Khan, M., Khan, R., Islam, S. U. et al. (2024a). Provenance, Diagenesis, and Depositional Environment of Miocene Kamlial Formation, Azad Jammu and Kashmir, Sub Himalayas, Pakistan: Evidences from Field Observations and Petrography. *Heliyon, 10,* e24309. https://doi.org/10.1016/j.heliyon.2024.e24309

Khan, M., Khan, R., Madayipu, N. et al. (2024b). Structural and Stratigraphic Study of Hazara-Kashmir Syntax, Pakistan with the Aid of Geographic Information System and Field Data Approach. *Journal of the Geological Society of India, 100,* 78-90.

Larsen, G., & Chilingarian, G. V. (2010). *Diagenesis in Sediments and Sedimentary Rocks* (Volume 2). Elsevier

Malkani, M. S. (2020). Mineral Resources of Gilgit Baltistan and Azad Kashmir, Pakistan:

An Update. *Open Journal of Geology, 10,* 661-702. https://doi.org/10.4236/ojg.2020.106030

Mughal, M. S., Zhang, C., Du, D. et al. (2018). Petrography and Provenance of the Early Miocene Murree Formation, Himalayan Foreland Basin, Muzaffarabad, Pakistan. *Journal of Asian Earth Sciences, 162,* 25-40. https://doi.org/10.1016/j.jseaes.2018.04.018

Shah, A. A. (2015). Kashmir Basin Fault and Its Tectonic Significance in NW Himalaya, Jammu and Kashmir, India. *International Journal of Earth Sciences, 104,* 1901-1906. https://doi.org/10.1007/s00531-015-1183-1

Shaheen, H., Qaseem, M. F., Amjad, M. S., & Bruschi, P. (2017). Exploration of Ethno-Medicinal Knowledge among Rural Communities of Pearl Valley; Rawalakot, District Poonch Azad Jammu and Kashmir. *PLOS ONE, 12,* e0183956. https://doi.org/10.1371/journal.pone.0183956

Singh, P., & Patel, R. C. (2022). Miocene Development of the Main Boundary Thrust and Ramgarh Thrust, and Exhumation of Lesser Himalayan Rocks of the Kumaun-Garhwal Region, NW-Himalaya (India): Insights from Fission Track Thermochronology. *Journal of Asian Earth Sciences, 224,* Article ID: 104987. https://doi.org/10.1016/j.jseaes.2021.104987

Ullah, K., Arif, M., & Shah, M. T. (2006). Petrography of Sandstones from the Kamlial and Chinji Formations, Southwestern Kohat Plateau, NW Pakistan: Implications for Source Lithology and Paleoclimate. *Journal of Himalayan Earth Sciences, 39,* 1-13.

Yasin, M., Ali, S. M. K., Munir, H., & Ishfaque, M. (2017). The Sedimentary Geology, Remote Sensing, Geomorphology and Petrology of Miocene to Late Pliocene Sediments in District Sudhunhoti and Poonch, Azad Jammu and Kashmir, Pakistan. *Earth Sciences Malaysia (ESMY), 1,* 8-14. https://doi.org/10.26480/esmy.01.2017.08.14

Zaheer, M., Khan, M. R., Mughal, M. S. et al. (2022). Petrography and Lithofacies of the Siwalik Group in the Core of Hazara-Kashmir Syntaxis: Implications for Middle Stage Himalayan Orogeny and Paleoclimatic Conditions. *Minerals, 12,* Article No. 1055. https://doi.org/10.3390/min12081055

Zhang, J., Santosh, M., Wang, X. et al. (2012). Tectonics of the Northern Himalaya since the India-Asia Collision. *Gondwana Research, 21,* 939-960. https://doi.org/10.1016/j.gr.2011.11.004